Large Scores and Radial Cracks on Case-Hardened Worms

Wolfgang Predki, Friedrich Jarchow, Ralf Dinter and Alexander Rhode

Abstract

In the last couple of years, many research projects dealt with the determination of load limits of cylindrical worm gears. These projects primarily focused on the load capacity of the worm wheel, whereas the worm was neglected. This contribution presents investigations regarding damages such as large scores and cracks on the flanks of case-hardened worms.

Introduction

The load-carrying capacity of cylindrical worm gears is generally limited by the worm wheel made of bronze. This material has a lower strength than the worm made of steel. Critical loads are reached if pitting, sliding wear, tooth breakage, scuffing or high oil temperatures occur. However, in the last couple of years, defects such as radial cracks or large scores have increased on the case-hardened worm surface. These defects can cause an increased wear on the worm wheel, which can lead to a premature loss of drive. This report shows a way to determine the maximum permissible load that leads to these defects, as well as testing new methods which increase the load carrying capacity.

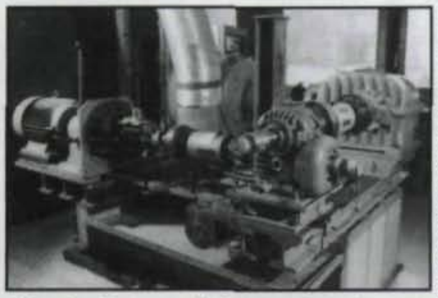

Fig. 1—Test stand for scoring damage, center distance a = 100 mm.

Fig. 2—Test stand for cracking damage, center distance a = 250 mm.

Fig. 3—Large score marks on a case-hardened worm.

Test Conditions

The test runs to examine score marks and cracks on hardened worm flanks were executed separately on two electrically strutted test stands. The mating materials are case-hardened worms made of 16MnCr5 steel and worm wheels made of GZ-CuSn12Ni bronze. Tests for scoring were executed with gear sets with a center distance of a = 100 mm, a gear ratio of i = 41:2, a worm shaft arranged below the worm gear and splash lubrication. Figure 1 shows the test stand that was employed for scoring tests.

After assembly and adjustment of the contact pattern, the worm gear sets were loaded immediately with the entire torque and run for 336 hours, without any running-in process. The rotational speeds of the tested worms were:

n_1 = 400; 650; 1,030 and 1,470 1/min.

The torque varied from 1.0 to 1.75 times the nominal torque that is given by the gear manufacturer (Ref. 7). Cracks on the worm flanks were tested on larger gear sets with a center distance of a = 250 mm, a gear ratio of i = 39:2, a worm shaft arranged above the worm gear and a combined splash/circulating lubrication with an external oil cooling system. That test stand is shown in Figure 2.

The testing period is limited to a maximum of 1,650 hours. The rotational speeds are 1,500 and 2,200 1/min. During the tests, the applied torque exceeds the nominal torque 1.75 and 2.00 times. The employed lubricant for each case is a polyglycol called FVA-reference-oil PG4 (Ref. 4) with additive combination LP1655.

Test Results: Scoring

Figure 3 illustrates a worm gear damaged by score marks. Compared to new, never-run worms, the flanks show a rough surface within the area of contact. These score marks are transferred during operation to the flanks of the worm wheel and cause excessively increased wear that often leads to a premature failure of the entire gear set.

In order to register the amount of scoring damage, measurements of the surface are carried out in the complete mating area of the worm shaft. The measurements are taken in the radial direction, perpendicular to the expected score marks (Fig. 4).

In the radial direction, parts of the teeth are separated into foot, center and tip. Tests with a low rotational speed of n_1 = 400 1/min and 1.25 times the nominal torque show the largest scoring damage. The distribution of the measured arithmetic mean roughness R_a after testing is given with Figure 5. The measured values for each position from the beginning to the end of the contact area are plotted. The roughness of the flanks in the initial state is the standard of comparison. New worms have an average arithmetic mean roughness of R_a = 0.4 µm.

The distribution shown is typical for worms that are damaged by score marks. The greatest roughness always occurs at the end of the contact area close to the tip of the tooth. Towards the beginning of the mating area, the values of the roughness decrease. Similar tendencies can be observed in the center of the teeth, but the maximum values are lower. In the area of the foot, the measured values scatter, but they reach comparatively large values.

Comparative measurements of the worm shaft and the worm wheel show a good representation of the scoring damage of the worm flanks by measurements at the wheel tooth center. At this point, the smallest lubricant film thickness and the smallest relative motions directed toward the height of the tooth occur during operation between worm and wheel.

Score marks of the worm are reflected onto the center of the wheel teeth. Therefore, score marks at the wheel are suitable for the qualitative description of the scoring damage at the worm flanks. Figure 6 shows the measured arithmetic mean roughness at the wheel after separate test runs with different loads. All tests were executed with case-hardened worms made with 16MnCr5 steel and wheels made of GZ-CuSn12Ni bronze.

The test results show a significant dependence on rotational speed and torque. The amount of scoring damage increases with an increase in the torque applied and decreases with the rotational speed of the worm shaft (Fig. 6). On the one hand, increased load leads to an increased scoring damage. On the other hand, an increased rotational speed leads to less scoring. The strongest scoring damage can be observed at rotational speeds of $n_1 = 400$ 1/min. At rotational speeds of more than $n_1 = 1{,}030$ 1/min, no score marks result, even in the case of high overloads. The roughness of the flanks after testing is almost the same as in the beginning. The arithmetic mean roughness represents the amount of scoring damage.

A regression analysis quantifies the dependence of the expected arithmetic mean roughness on the worm wheel on different loads as rotational speed n_1, torque T_2 and oil sump temperature ϑ_S by four coefficients $a_{1\text{-}4}$.

$$R_{a,R} = a_1 + (a_2 - a_3 \cdot n_1 + a_4 \cdot \vartheta_S) \cdot T_2 \geq 0\,\mu\text{m} \quad (1)$$

Figure 7 shows the expected arithmetic roughness $R_{a,R}$ after application of Equation 1. A data map shows the expected scoring damage for the examined material-lubricant combination depending on torque and rotational speed.

As observed during the tests, the roughness increases with increasing load and decreasing rotational speed. Measurements during the testing reveal an increased wear for $R_{a,R} = 1\text{–}2\ \mu$m, and excessively increased wear if greater roughness applies. In some cases, the measured wear exceeds the values precalculated by DIN 3996 (Ref. 3) up to 20 times. For this reason, an arithmetic mean roughness above $R_a = 2\ \mu$m has to be particularly regarded as critical. For operation with constant torque directly after gear set assembly, the loads should be chosen in a way that the expected arithmetic mean roughness stays below 1 µm, in order to avoid damaging score marks.

The presented approach can only be used to predict the behavior of the tested material/lubricant combination and the given geometry of the gearset. A prediction for operating points which are not represented by the examined range of torque and rotational speed is highly uncertain and not verified by practical investigations. A transfer of the results to different sizes and another tooth geometry just by conversion of the dependent factors n_1, T_2, ϑ_S to other factors such as sliding velocity v_{gm} and mean contact stress σ_{Hm} lack of test results for these conditions.

Methods to Avoid Score Marks

Scoring on the worm flanks can be avoided by the use of PVD-coated worms such as those coated with BALINIT C (Ref. 1) or the use of the additive GH6. Compared to the basic test runs, even higher torques can be applied. No score marks appear during these tests. Concerted oil changes after 48 and 144 hours help to reduce the scoring damage. However, scoring cannot be avoided completely by this particular means.

Compared to the basic gear sets, no

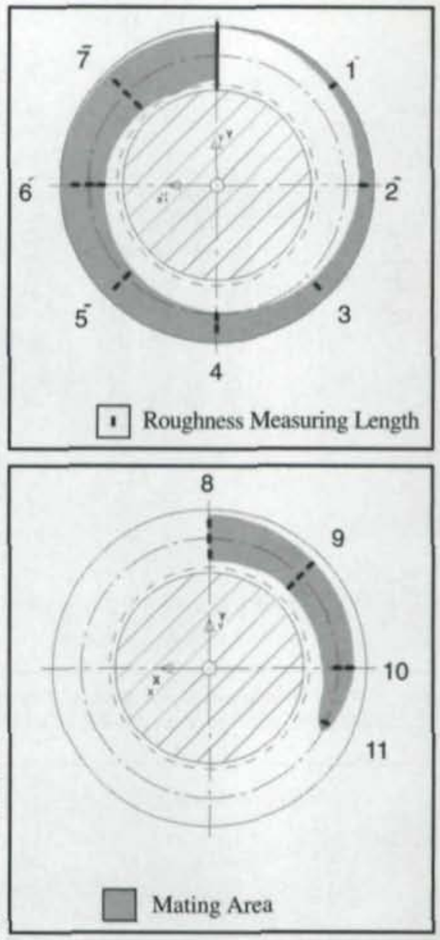

Fig. 4—Positions where measurements of the surface are taken to represent scoring damage.

Prof. Dr.-Ing. Wolfgang Predki
is the head of the chair of mechanical components, industrial and automotive power transmission at Ruhr University, located in Bochum, Germany. The chair's research focuses on wear optimization of worm gears, plastic and sintered worm gears and bronze optimization.

Prof. em. Dr.-Ing. Friedrich Jarchow
is the former head of the chair of mechanical components, industrial and automotive power transmission at Ruhr University.

Dr.-Ing. Ralf Dinter
is employed at Winergy AG, a leading provider of drive systems for wind turbines, located in Voerde/Friedrichsfeld, Germany. Winergy AG is a subsidiary of A. Friedr. Flender GmbH, based in Bocholt, Germany.

Dipl.-Ing. Alexander Rhode
is a research assistant at the chair of mechanical components, industrial and automotive power transmission at Ruhr University. His work focuses on the investigation of large scores on worms.

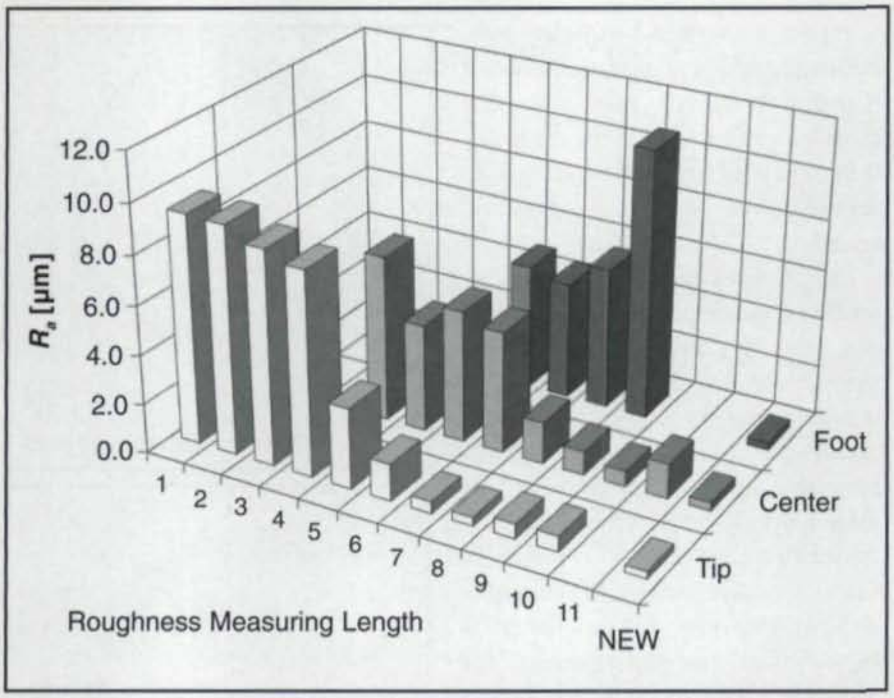

Fig. 5—Arithmetic mean roughness after testing (336 hours), n_1=400 1/min, T_2 = 1.25 • T_{2N}, 16MnCr5 case-hardened/GZ-CuSn12Ni.

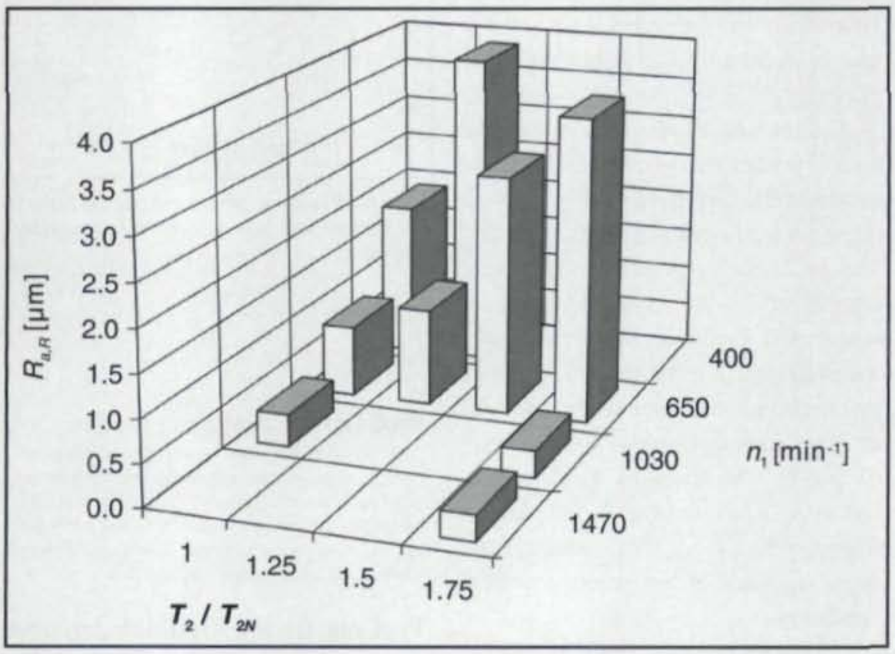

Fig. 6—Arithmetic mean roughness of the wheel after 336 hours.

improvement should be expected by the application of polished or crowned worms made of 16MnCr5 case-hardened steel. Spalling can be observed within the nitrided fringe of gas nitrided worms.

Test Results: Cracking

Radial cracks on the flanks of case-hardened worms can be encountered on gear sets with center distances above a = 200 mm, but they predominantly occur with center distances above a = 400 mm. High sliding speeds and incomplete starting contact patterns lead to high specific loads on the tooth flanks of these gear drives. For economical bench tests, gear drives of the size a = 250 mm were examined. These drives were charged with overloads up to twice the nominal torque.

Figure 8 shows a bar chart that sums up the results of several tests. The testing period is represented by the length of each bar. Different hatching indicates several defects on the worm flanks. The employed worm materials as well as the hardening processes are given with this figure.

The nominal torque must be exceeded by far to produce cracks. High loads lead to heavy pitting and, in some cases, excessive wear on the worm wheels. The cracks on the worm flanks always occur at the end of the mating area and show a radial alignment. There are two different areas for the origin of the cracks and their direction of growth. On the one hand, cracks start at the inner delimitation of the contact field with a growth direction towards the tip of the worm tooth (Fig. 9). On the other hand, cracks start at the tip and grow towards the tooth (Fig. 10). For both cases, the origin of the cracks is located within an area of disadvantageous lubrication conditions. After the tests, a local transfer of bronze can be observed in these areas.

Theoretical examinations (Refs. 2, 6) show the smallest lubricant film thickness at the inner delimitation of the worm mating area. Compared to other areas on the flank, higher friction factors apply for this region. The combination of high friction factor and the existing speeds lead, particularly towards the end of the mating area, to high temperatures on the flank.

Cracks that start at the tip of a worm tooth can be observed if large pitted areas are located on the wheel teeth and increased wear commences. The tooth face tip of the worm "digs" into the foot of the wheel tooth. The development of a sufficient lubricating film in this area is restrained by the sharp-edged tip of the worm tooth and the prevailing conditions of motion.

A theoretical analysis of the mating process shows a contact or wear between the tip of the worm tooth and the foot of the wheel tooth at the end of the worm mating area, which corresponds to the test results.

As metallographic examinations

show, the flanks of the worm were stressed by very high temperatures within the mating area. The fringe texture is thermally influenced. Even rehardening of the flank surfaces occurred. Rehardening requires temperatures above the austenite temperature of at least a_{Cl} = 723°C.

Internal stress analyses reveal that the loads applied to the worm flanks lead to high tensional internal stresses within the fringe. A new worm shows compressive internal stresses within the same areas.

The change in the state of internal stresses by high surface temperatures is shown in Figure 11. In this example, there is no internal stress at the beginning. A short application of a temperature field to the surface of a part causes compressive stresses within areas close to the surface because a free, temperature-caused extension is prevented by the surrounding colder areas. An increase of the temperature causes higher compressive internal stresses. If these stresses reach the hot-strain limit, permanent strains occur. The value of the hot strain-limit depends on the temperature. After removal of the thermal stress, the deformed area cools down and the strains are saved as tensional internal stresses. Hertzian contact stresses and tangential loads caused by friction promote this effect. If the local strength of the material is exceeded by tensional internal stresses, the growth of a crack commences.

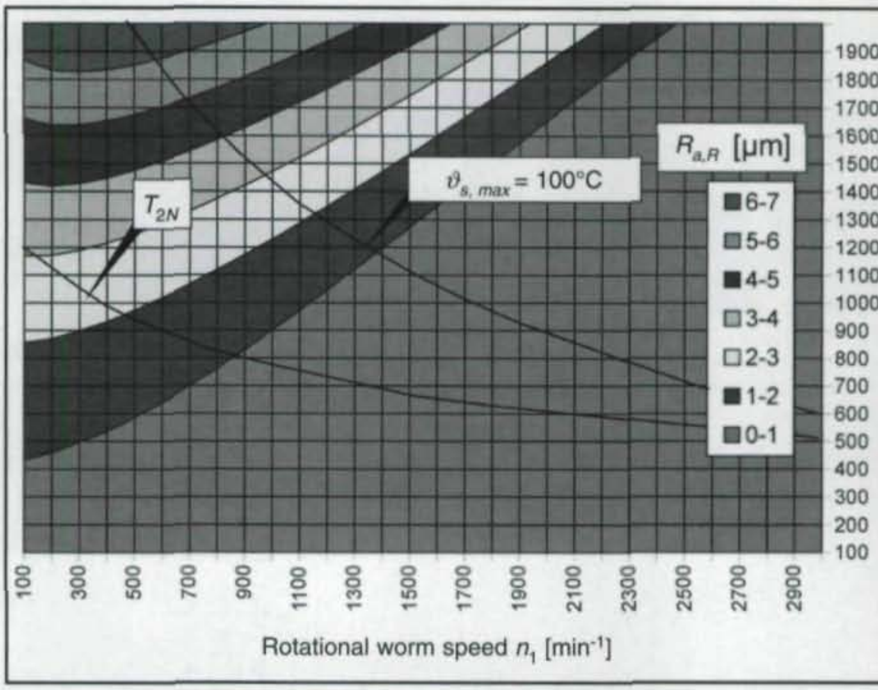

Fig. 7—Estimated scoring damage, calculated by Equation 1. Gear set: a = 100 mm, i = 20.5, 16MnCr5eh/GZ-CuSn12Ni, operation with nominal load, no running-in, nominal torque T_{2N} taken from manufacturer data (Ref. 7).

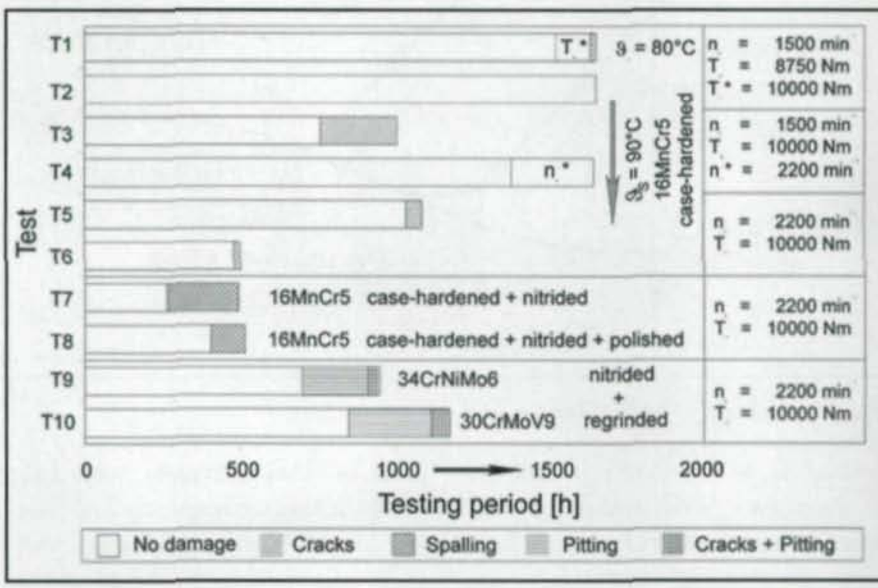

Fig. 8—Test results cracking. Wheel is GZ-CuSn12Ni; lubricant: FVA-PG4 + LP1655

Test Conclusions

The nominal torque has to be exceeded by far to produce cracks on the worm flanks. For this reason, these defects should not be expected under normal working conditions with worm gear drives of the tested size. The defects are caused by high thermal loads in combination with a local transfer of bronze. In particular, cracks occur in combination with heavily pitted worm wheels.

That is another reason why pitting should be avoided. Gas nitrided worms tend to spall within the nitrided layer.

In order to reduce the risk of cracks on case-hardened worms, the specific load on the flanks should be reduced and the load-capacity against scuffing should be increased. In general, this can be reached by the following means:

- Largest possible starting contact pattern;
- Fast running-in by use of a bronze with low strength in combination with a mineral oil, subsequent oil change and use of a more efficient polyglycol;
- Use of a lubricant with high load-capacity against scuffing in order to prevent local transfer of bronze;
- Prevention of pitting on the worm wheel (for precalculation, see Ref. 5).

Conclusions

This research project explores the critical loads of hardened worms that are combined with wheels made of bronze. Two different types of defects, large scores and radial cracks, are examined separately.

A map for score damage can be created. It shows that an increased amount of

Fig. 9—Worm taken from test T3. Origin of the crack at the inner delimitation of the contact field (cracks redrawn for better illustration).

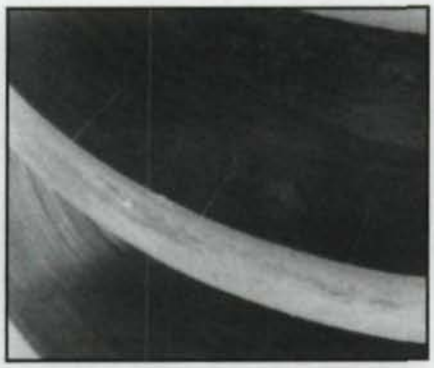

Fig. 10—Worm taken from test T1. Origin of the crack at the tip of the tooth.

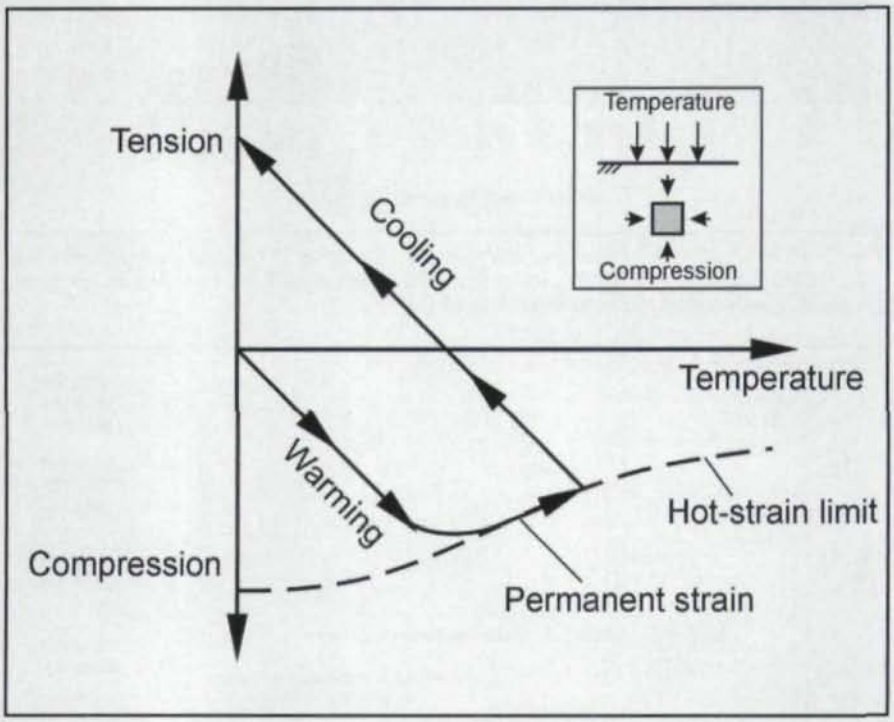

Fig. 11—Changes of internal stresses by thermal loads.

scoring is to be expected with an increased load. An increase in rotational speed reduces the expected damage. However, even high overloads do not produce score marks if high rotational speeds apply. An effective way to prevent scoring is the use of PVD-coated worms or the use of a lubricant with the additive GH6.

To generate cracks on the worm flanks, the nominal torque must be exceeded greatly. For this reason, cracks are not to be expected under normal working conditions with worm gear drives of the tested size. The defects are caused by high thermal loads in combination with a local transfer of bronze. The origin of the cracks is located within areas of disadvantageous lubrication conditions and consequently high thermal loads. Material tests showed thermally-influenced fringe texture and, in some cases, even zones where rehardening occurred.

Internal stress analyses indicate a change from initially compressive to high tensional internal stresses, caused by high flash temperatures. These stresses lead to cracks, if the local strength of the material is exceeded. In particular, cracks occur in combination with heavily pitted worm wheels. That is another reason why pitting should be avoided.

Further information can be obtained from the final report on research project 237 of the FVA (Ref. 5). ○

This paper was printed with the permission of the publisher from VDI-Gesellschaft Entwicklung, Konstruktion, Vertrieb (Ed.): International Conference on Gears, Vol. 1. VDI-Berichte 1665. Düsseldorf: VDI-Verlag 2002, pp. 435–449.

References

1. Balzers AG: "Firmenschrift", *Der Weg zu zuverlässigeren Bauteilen*, Liechtenstein 1993.

2. Bouché, B.: *Reibungszahlen von Schneckengetrieben im Mischreibungsgebiet*, Dissertation Ruhr-Universität Boch-um. 1991.

3. DIN-Entwurf 3996: *Tragfähigkeitsberechung von Zylinder-Schneckengetrieben mit Achsenwinkel Σ=90°*, Entwurf 1/95.

4. FVA-Forschungsheft 316: *Synthetische Referenzöle, Datensammlung für Syntheseöle*, 1990.

5. FVA-Arbeitsblatt zum Forschungsvorhaben Nr. 12/IV: *Versuche zur Grübchentragfähigkeit von Schneckengetrieben*, Stand Juni 1996.

6. FVA-Forschungsvorhaben 237. *Schneckentragfähigkeitsgrenzen ermitteln und erhöhen*, Heft 518 der Forschungsvereinigung Antriebstechnik, 1996.

7. Katalog der Firma Thyssen: *MUTAX Schneckenradsätze*, 1-750.

8. Klüber Firmenschrift: *Klübersynth GH6-Öle*, Produktinformation 5.118d, Ausgabe 03.93.

9. Predki, W.: *Hertz'sche Drücke, Schmierspalthöhen und Wirkungsgrade von Schneckengetrieben*, Dissertation Ruhr-Universität Bochum, 1982.